Utilization of Waste Grooved Razor Shell (GRS) as a Catalyst in Biodiesel Production from Refined and Waste Cooking Oils

Abdellah Aitlaalim [1], Fatiha Ouanji [1], Abdellah Benzaouak [2], Mohammed El Mahi [2], El Mostapha Lotfi [2], Mohamed Kacimi [1,*] and Leonarda Francesca Liotta [3,*]

[1] Laboratory of Physical Chemistry of Materials and Catalysis, Department of Chemistry, Faculty of Sciences, Mohammed V University in Rabat, Maroc B.P, 8007 N.U., Morocco; aitlaalim@hotmail.com (A.A.); fatiha.ouanji@gmail.com (F.O.)

[2] Laboratory of Spectroscopy, Molecular Modeling, Materials, Nanomaterials, Water and Environment, Environmental Materials Team, ENSAM, Mohammed V University in Rabat, Maroc B.P, 8007 N.U., Morocco; abdellah.benzaouak@um5.ac.ma (A.B.); m.elmahi@um5s.net.ma (M.E.M.); lotfi58@yahoo.fr (E.M.L.)

[3] Istituto per lo Studio dei Materiali Nanostrutturati (ISMN)-CNR, via Ugo La Malfa, 153, 90146 Palermo, Italy

[*] Correspondence: kacimimohammed@fsr.ac.ma (M.K.); leonardafrancesca.liotta@cnr.it (L.F.L.); Tel.: +39-091-6809371 (L.F.L.)

check for updates

Abstract: Biodiesel is a potential alternative for fossil fuel. However, its large-scale application is held up by the disadvantage of a homogenous process, the scarce availability of raw materials and the production cost, which is higher than for fossil diesel. In this work, biodiesel production was carried out using both refined and used cooking oils. The process was investigated in a batch reactor, in the presence of CaO as a heterogeneous catalyst prepared by the calcination of the natural Waste Grooved Razor Shell (GRS). Characterizations by X-Ray Diffraction (XRD) and Thermal Gravimetric (TG)/Differential Thermal Analysis (DTA) showed that the as-received GRS consists of aragonite, (i.e., $CaCO_3$) as the main component and of water and organic matter in a lower amount. After calcination at 900 °C, CaO was formed as the only crystalline phase. The effects of several experimental parameters in the transesterification reactions were studied, and their impact on the produced biodiesel properties was investigated. The studied variables were the methanol/oil molar ratio, the catalyst weight percentage (with respect to the oil mass), the calcination temperature of the parent GRS and the recycling and regeneration of the catalyst. The physico-chemical and fuel properties, i.e., viscosity, density and acid value of used oils and of the produced biodiesel, were determined by conventional methods (American Society for Testing and Materials (ASTM) methods) and compared with the European standards of biodiesel. The optimal identified conditions were the following: the use of a 15:1 methanol/oil molar ratio and 5 wt% of CaO with respect to the oil mass. After 3 h of reaction at 65 °C, the biodiesel yield was equal to 94% and 99% starting from waste and refined oils, respectively.

Keywords: waste grooved razor shell; biodiesel; transesterification; CaO catalyst; recycle and regeneration

1. Introduction

Earth is increasingly affected by several disasters, such as hurricanes, prolonged droughts and severe floods, that are related mainly to global warming, which is mostly the result of fossil fuels usage [1]. Human daily activities contribute deeply to the modification of the natural environmental equilibrium, causing severe climatic changes [2].

Today's civilization is on the threshold of a critical transition, as over the next 50 years it is expected that there will be the largest increase in energy demand that has ever occurred in history. This is due to both an increase in the world's population and the improvement of living standards in some developing countries. Rapid growth in energy needs will be difficult to bear in the medium term by the currently known reserves of fossil fuels (oil, coal and natural gas) [3,4].

Most of the energy consumed in the world comes from oil, coal and natural gas. However, the world has been looking for new alternatives for the energy matrix, and, with this, the natural sources of biomass are a viable alternative. Therefore, there is an increasing incentive to develop technologies allowing the use of renewable energy sources that are ecologically sound and economically viable.

Biodiesel, a mixture of fatty acid methyl esters (FAMEs), is defined as fuel obtained from natural renewable sources, and it can be used in diesel cycle engines [5]. It has been used in blends with fossil diesel, and the amounts used have been steadily increasing worldwide [6]. Its combustion does not release more CO_2 than the amount consumed during the photosynthesis process [7].

The production of biodiesel is currently carried out using the transesterification of vegetable oils and animal fats [8–12]. The industrial production of biodiesel is principally based on homogeneous catalysis in basic media. This process has the disadvantage of using acid for the neutralization of the base excess [13–15], with consequent environmental damage caused due to the byproducts formed. It is, therefore, imperative to implement a process for sustainable diesel production.

The synthesis of biodiesel can also be performed by heterogeneous catalysis. Such a strategy offers technical and environmental advantages over homogeneous catalysis, as it facilitates the purification of alkyl monoesters, allows the recycling of solid catalysts throughout their useful life and minimizes the generation of effluents. Besides, it considerably facilitates glycerin recovery and purification [14,16,17]. Several solids have been proposed as potential catalysts for biodiesel synthesis. The performance of these materials as catalysts is related to the nature of basic sites [18]. Calcium oxide is the most studied catalyst. Besides its basic properties, it has several other advantages, such as being available everywhere, easily recyclable, cheap and non-toxic [18]. However, similarly to many other catalysts, CaO suffers from lixiviation, which inexorably induces a loss of efficiency [14,17,18]. Moreover, calcium oxide reacts with water and CO_2, which lead respectively to lime and calcium carbonate, which are significantly less active than the corresponding oxide [19].

The investigations of marine or earth sources of calcium-based shells have attracted attention for many applications [20,21]. The majority of such shells consist of about 96% aragonite, that is $CaCO_3$ mineral, along with other components, such as organic substances and traces of SiO_2 and MgO oxides [22,23].

Thus, marine shells can be considered as sources of heterogeneous catalysts for biodiesel production [20,24].

The main goal of the present work is the preparation of CaO starting from Grooved Razor Shell (GRS). The resulting catalyst was characterized by different techniques, such as XRD, (Fourier Transform-Infrared (FT-IR), TG/DTA and SEM and investigated in the transesterification reaction of refined oils and used cooking oils for biodiesel production. The obtained results contribute to the valorization of marine resources, such as GRS, as a natural source of calcium oxide.

2. Results and Discussion

2.1. Materials Characterization

Figure 1 displays the XRD patterns of the GRS material before and after calcination at 900 °C. Before calcination, the diffraction pattern (Figure 1a) shows that the crystal structure of the shell sample is aragonite, a variety of the calcium carbonate, $CaCO_3$, phase according to JCPDS (Joint Committee on Powder Diffraction Standard) file N°00-005-0453 [23,25]. After calcination of the GRS sample at 900 °C for 1 h (heating rate 10 °C·min^{-1}), diffraction peaks appeared at 2θ = 32.26, 37.44, 53.9° (Figure 1b), which are characteristic of CaO (JCPDS N°00-02-0968) [23]. Such a temperature was selected as a

suitable calcination temperature to produce the CaO catalyst from the GRS shell according to the TG/DTA analysis.
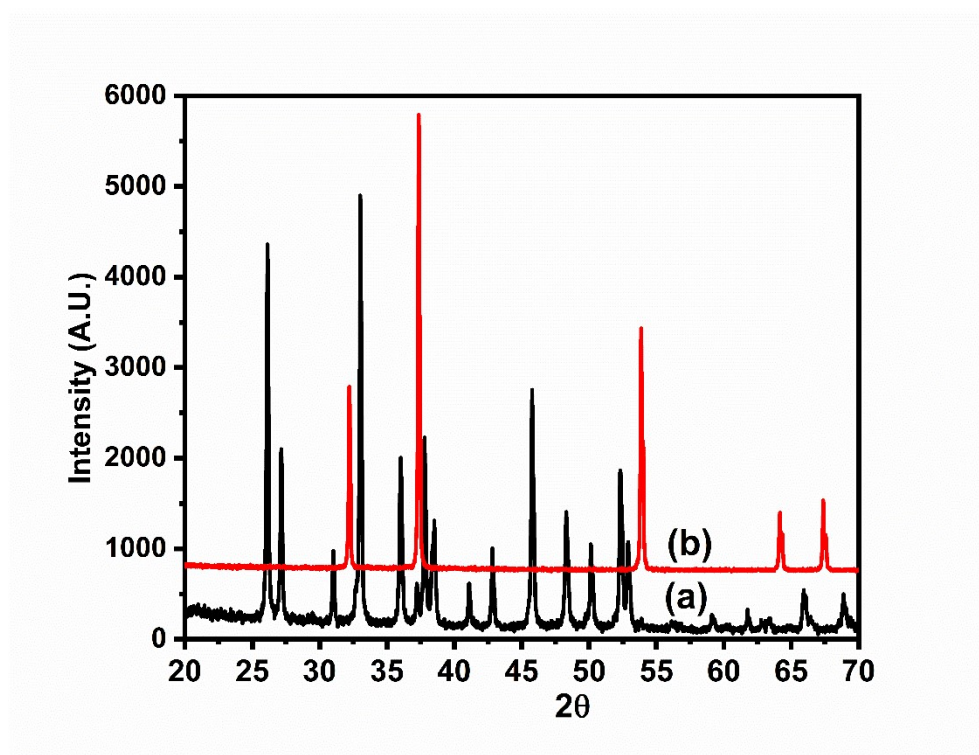

Figure 1. XRD patterns for the (**a**) natural GRS shell and (**b**) calcined GRS shell at 900 °C.

The FT-IR spectrum of the GRS powder is displayed in Figure 2, curve a. The spectrum shows bands located at 1445, 1083 and 857 cm^{-1} attributed to $\nu 1$, $\nu 2$ and $\nu 3$ vibration modes of carbonate ions that are typically found in aragonite polymorph calcium carbonate [26]. In addition, the doublet at 699 and 712 cm^{-1} was assigned to the $\nu 4$ vibration mode of carbonate ions. The small band observed at 1789 cm^{-1} is due to the C=O stretching vibration [23,26]. The presence of water molecules in the un-calcined sample was confirmed from the broad peak which appeared at around 3270 cm^{-1}. In Figure 2, curve b is the spectrum of the GRS shell after calcination at 900 °C. It is worth noting that the easily formed CaO reacts with the moisture and CO_2 present in the atmosphere. Accordingly, the strong peak at 3640 cm^{-1} was attributed to strongly chemisorbed water or to OH groups [23]; additionally, the two bands at 2979 and 2890 cm^{-1} were ascribed to the stretching of perturbed OH groups [27]. The bands at 1460, 1410, 1245, 1063 and 872 cm^{-1} were assigned to the C–O stretching and bending, ν_1, ν_2, ν_3 and ν_4 vibration modes, respectively, of calcium carbonate species formed upon CO_2 adsorption on CaO [23,26].
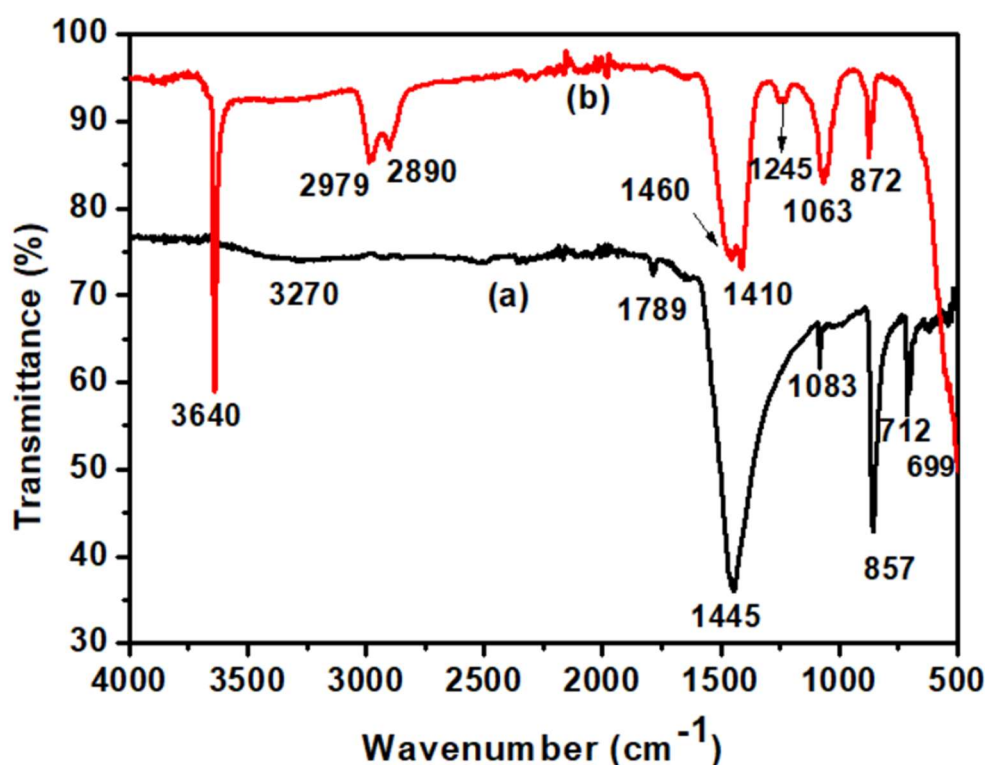
Figure 2. FT-IR curves for the (**a**) GRS shell and (**b**) calcined GRS shell at 900 °C.

Simultaneous TG-DTA analyses were performed in order to investigate the suitable calcination temperature to obtain a pure CaO catalyst from GRS. As has been shown in Figure 3, the TG curve shows a weight loss between 200–400 °C, which was associated with the elimination of water and the organic components typical of the natural shell. The corresponding weight loss is about 3%. According to the literature [23] and as shown by XRD patterns recorded upon the temperature programmed oxidation treatment at different temperatures under air flow (see the experimental part for details and results, in Supplementary Materials, Figure S1), the formation of calcite, another mineral form of $CaCO_3$ (JCPDS N°01-086-2339) and the disappearance of the aragonite phase occur. A second weight loss (~40%) was observed in the range of temperature between 600–860 °C. Then, above 860 °C, the weight of the sample remained constant. The heat flow curve measured by DTA shows a main endothermic peak at 845 °C corresponding to the minimum of the DTG curve, which was attributed to the transformation of calcite into CaO, in agreement with the XRD patterns (Figure 1, curve b, and Supplementary Materials, Figure S1).

The morphological features of the un-calcined GRS shell and of the resulting material after calcination at 900 °C were studied by Scanning Electron Microscopy (SEM). The un-calcined GRS shell exhibits rod and spherical particles with irregular sizes (see Figure 4a). After calcination at 900 °C (see Figure 4b), agglomerated irregular particles are visible; moreover, a macro-porous structure appears, with many voids and intraparticle spaces, likely due to the evolution of gaseous species, such the release of water, organic matter and CO_2 due to the decomposition of $CaCO_3$ to CaO.

The EDS analysis of shells shows that Ca and O are the main components, in both uncalcined and calcined shell samples. The Ca content ranged between 21.57 and 25.12 at % for uncalcined and calcined shells, while the O content varied between 64.58 and 68.89 at %. Traces of Na (0.46 at %) were detected in the uncalcined sample. In both materials, carbon was present at 13.38 and 5.99 at % in the uncalcined and calcined shell, respectively. In the uncalcined GRS, the carbon was ascribed to the organic matter and also to carbonates, detected also in the calcined material (see FT-IR spectra, Figure 2). Moreover, the contribution of the carbon grid used for sample deposition cannot be excluded.
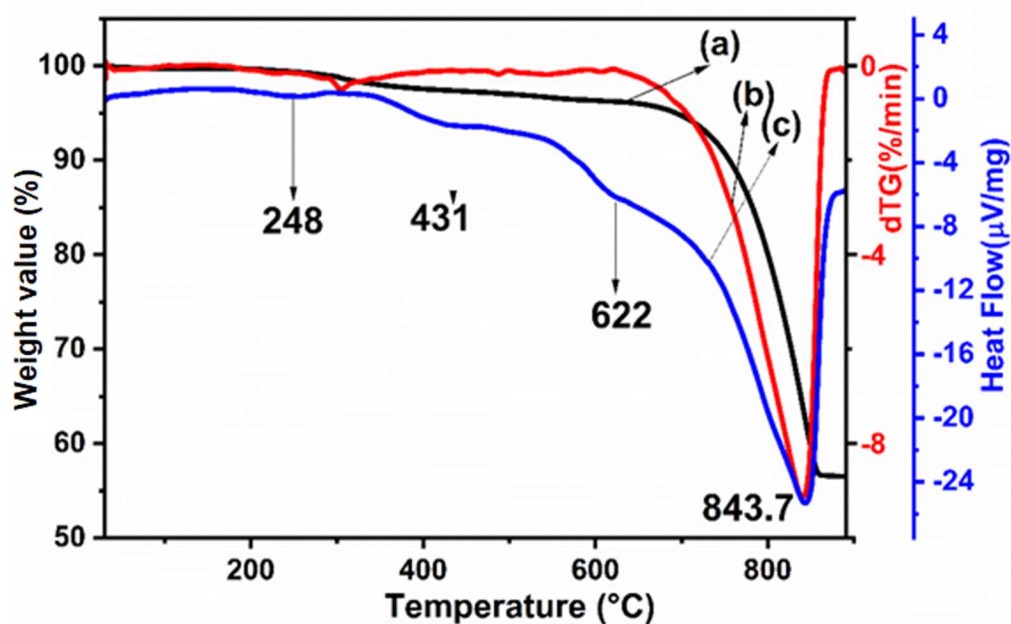
Figure 3. (**a**) TG, (**b**) DTG and (**c**) DTA curves under air flow for the GRS shell.
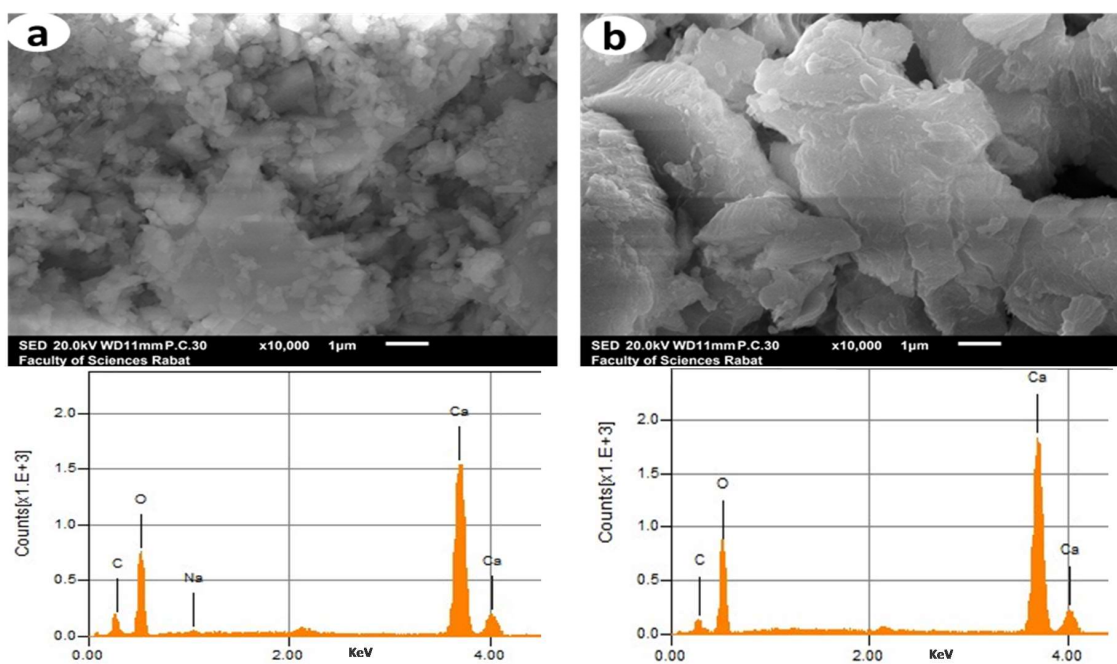

Figure 4. SEM morphology and EDX analysis of (**a**) the uncalcined GRS shell and (**b**) the resulting material calcined at 900 °C.

2.2. Oil Characterization

The oils used in this work were a refined cooking oil purchased from a local supermarket and a waste cooking oil, collected from the University Restaurants of Rabat, Morocco, respectively. In Table 1, the physical properties and fatty acid methyl esters weight composition of the refined and used oils are listed. The most abundant fatty acid is the linoleic acid methyl ester (C18:2), with percentages of ~57.4% and ~53.9% in refined and used oils, respectively.

Table 1. Physical properties and fatty acid methyl esters composition of refined and used frying oils.

Properties	Units	Refined Frying Oil	Used Frying Oil
Viscosity (40 °C)	cSt	33.5	36.6
Density (20 °C)	g/cm^3	0.921	0.960
Acidic value	mg KOH/g	0.27	1.32
Fatty acid type	Carbon chain	Composition (wt%)	
Myristic	C14:0	-	0.16
Palmitic	C16:0	9.79	10.24
Palmitoleic	C16:1	traces	traces
Stearic	C18:0	3.66	3.85
Oleic	C18:1	23.0	28.87
Linoleic	C18:2	57.36	53.86
Linolenic	C18:3	6.19	3.02

Table 1 also reports the viscosities, densities and acid values of the studied oils. The used oil has a relatively higher acidic value than the refined one (1.32 vs. 0.27) as a consequence of the hydrolysis of the triglycerides during the frying process. However, the acidic value of the used oil is still below the critical FFAs concentration requested to prevent the alkali-catalyzed transesterification [7,28,29]. The physico-chemical properties of the used oil are dramatically modified because such oil was used for fish frying, and it was replaced each day, collecting above 1900 to 2000 L/month.

The infrared spectra (Figure 5) for refined and used cooking oils were similar. The main absorption bands can be observed: CH stretch of alkene at 3008 cm^{-1}; CH_2 alkane stretch at 2922 and 2853 cm^{-1}; carbonyl stretch C=O at 1743 cm^{-1}; angular deformation of alkane CH at 1462 and at 1370 cm^{-1}; stretching of the C-O ester bond at 1160 cm^{-1} and asymmetric angular deformation of CH at 725 cm^{-1}, characteristic of long hydrocarbon chains $(CH_2)_n$.
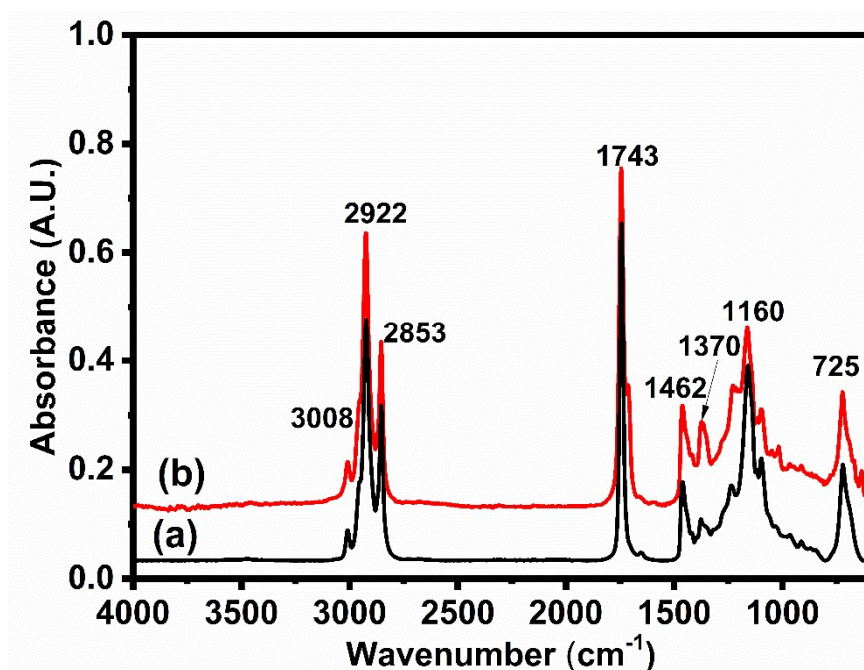
Figure 5. FT-IR spectrum of (**a**) refined cooking oil and (**b**) waste cooking oil.

The ^{1}H-NMR spectra of the refined and used oils are also similar, as shown in Figure 6. The two spectra clearly indicate signals at 4.05–4.38 ppm (OCH$_2$; sn-1, sn-3), 5.25 ppm (OCH; sn-2) due to the glycerol fraction, 5.05–5.5 ppm (CH=CH), 2.6–2.9 ppm (bisallylic, CH=CH–CH$_2$–CH=CH), 2.1–2.5 ppm (CH$_2$C=O), 1.9–2.1 ppm (allylic, CH$_2$–CH=CH–) and 1.61 ppm (CH$_2$–CH$_2$C=O); 1.24 ppm

and 1.30 ppm correspond to the alkyl group $(CH_2)_n$, and those at 0.75–1.0 ppm are characteristic of terminal CH_3 triglycerides comprising both a saturated and unsaturated fatty acid chain [7,30].
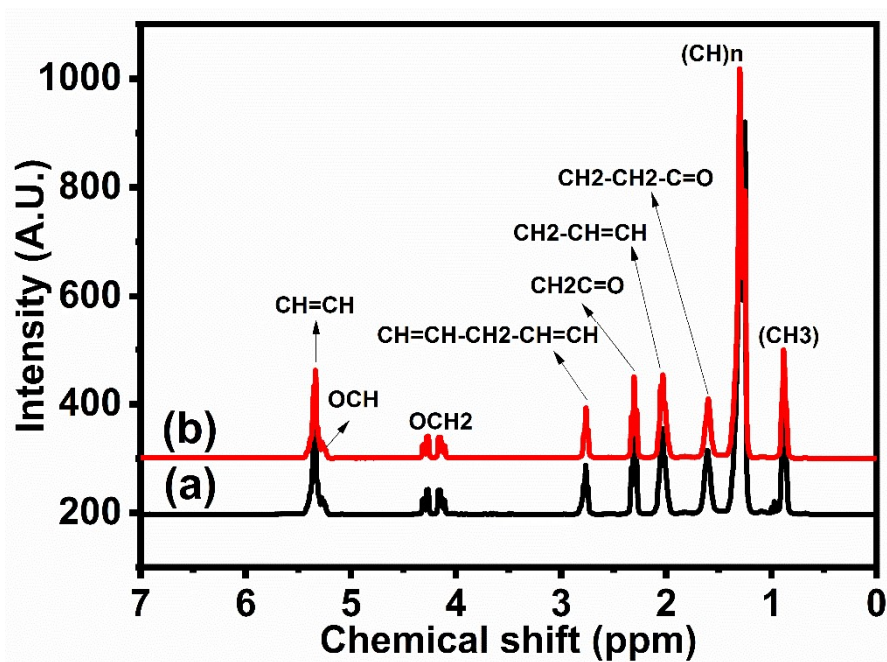

Figure 6. ^{1}H-NMR spectra of (**a**) refined cooking oil and (**b**) waste cooking oil.

The application of a thermogravimetric analysis has been widely reported in the literature as a useful technique for the characterization of oils, as well as of derived biodiesels [31]. Figure 7 reports the TG/DTG results for the refined and used oils investigated in the present article. The weight curve of the two oil samples started to significantly decrease at around 375 °C, and it continued until total degradation at 445 °C (see DTG curves a', b'). However, the waste oil curve presented an additional first small loss at 290 °C (Figure 7, curves b, b') that was assigned to the oxidation of free fatty acids that are formed during frying. Thus, although the thermogravimetric profiles of the refined and waste oils are quite similar, the small feature at around 300 °C is an important characteristic that depends on the free fatty acids content; therefore, TG/DTG is a helpful method for discriminating between mixtures of different oils.
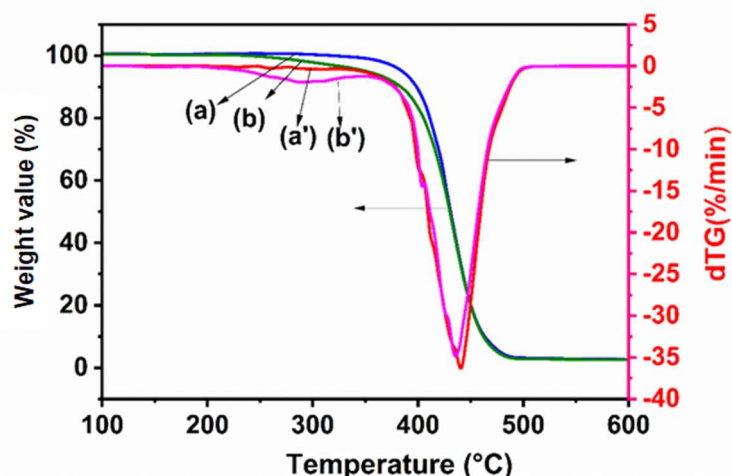

Figure 7. TG/DTG curves under air flow for refined oil (**a,a'**) and waste oil (**b,b'**).

2.3. Catalytic Activity

Calcium oxide, CaO, is known as an efficient transesterification catalyst [32]. It is not expensive and can be recycled. The cockle shell (Anadara granosa), which is available in abundance, has been reported as a source of calcium oxide and has been used as a catalyst for the transesterification reaction to produce biodiesel [33]. In the present work, we have considered it attractive to investigate another shell type (GRS) as a source of CaO for the transesterification reaction, and we have evaluated the optimal reaction conditions for biodiesel production. It is well known that biodiesel yield depends on several factors, such as the molar ratio of methanol to oil, amount of catalyst, time and reaction temperature [7]. In this study, particular attention was paid to the effect of the methanol/oil ratio because of its influence on the cost of the biodiesel product [7]. The reaction time was fixed at 3 h, a longer reaction time resulting in the hydrolysis of esters, forming soap [24]. The reaction temperature was set at the boiling point of methanol, 65 °C. The molar ratio of methanol to oil was varied from 3:1 to 18:1 for different catalyst amounts.

2.3.1. Effect of Methanol/Oil Molar Ratio

Figures 8 and 9 display the results obtained in the transesterification reaction of waste and refined oils, respectively, working at different weight contents of the catalyst with respect to the oil, in the range of 1.5 to 5 wt%. The conversion of the waste oil increased by increasing the methanol/oil molar ratio up to 12:1 and remained stable at 15:1. At a given methanol/oil ratio, the conversion values increased by using a higher amount of catalyst, with the highest conversion, equal to 94%, achieved in the presence of 5 wt%. At a methanol/oil molar ratio of 18:1, the conversion diminished to ~91% with 5 wt% of catalyst, while a value of 87% was registered by using the lowest amount of catalyst, 1.5 wt%.
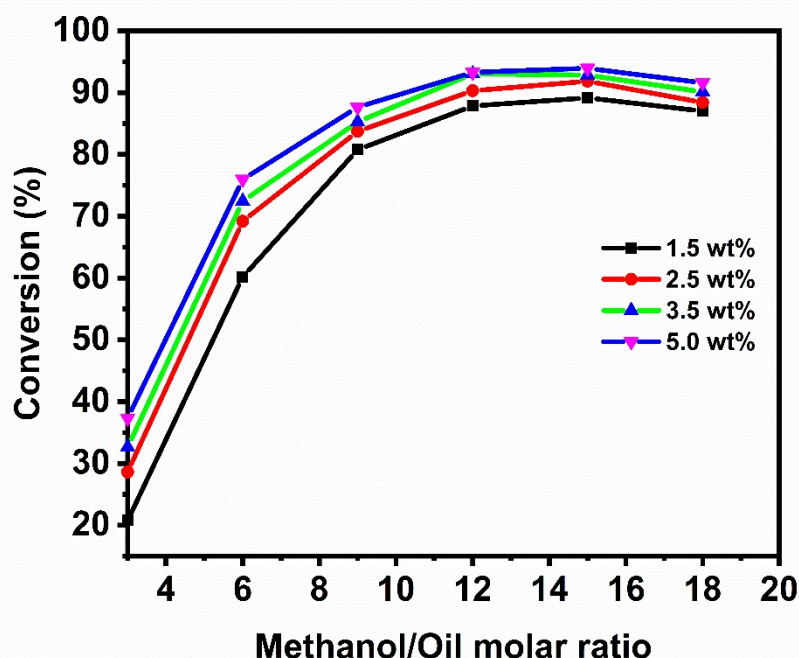

Figure 8. Effect of the molar ratio methanol/waste oil on the biodiesel production at different catalyst weight loadings and a reaction temperature of 65 °C.
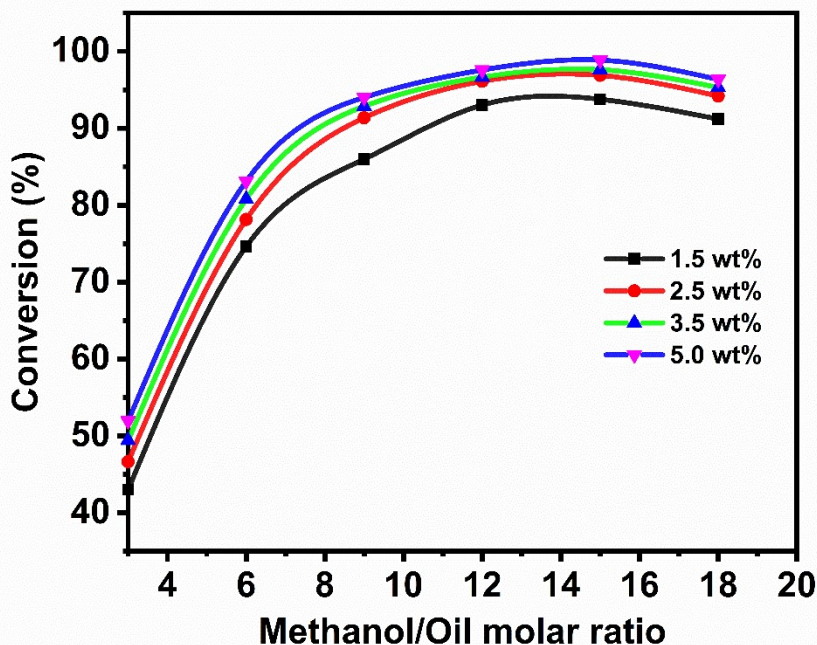
Figure 9. Effect of the molar ratio methanol/refined oil on the biodiesel production at different catalyst weight loadings and a reaction temperature of 65 °C.

A similar trend and higher conversions were registered by using the refined oil (Figure 9). In such a case, the highest value of conversion, 99%, was achieved at a molar ratio of 15:1 with 5 wt% of catalyst, while slightly lower conversions were registered at 12:1 and at 18:1, ~98% and 96.5%, respectively.

In conclusion, based on our results, 15:1 is the ideal methanol:oil ratio in the transesterification reaction using CaO obtained from calcined GRS.

Similar results have been observed in the majority of previous studies concerning the use of heterogeneous CaO-based catalysts [33]. It is important to note that the adequate methanol/oil ratio in homogeneous conditions ranges between 6–8:1, while in heterogeneous conditions where the reaction mixture forms a three-phase system, catalyst-oil-methanol, higher methanol:oil ratios are required in order to overcome the resistance to diffusion between different phases and shift the equilibrium towards product formation [34]. The use of an alcohol/oil ratio superior to the stoichiometric one has a significant effect on the biodiesel production cost [35]. Indeed, the polar hydroxyl groups of methanol acting as an emulsifier lead to the formation of gels, resulting in a difficulty of separation and purification of methyl ester [36].

Based on the results that have been reported so far, which fixed the best experimental conditions for the biodiesel yield at a methanol/oil molar ratio of 15:1, reaction temperature of 65 °C (boiling point of methanol) and reaction time of 3 h, the effect on the triglycerides conversion of the catalyst amount (wt% with respect to the oil) was investigated. The catalyst amount, as CaO derived from GRS, varied from 0.5–5% of the oil weight, and the results are shown in the Supplementary Materials, Figure S2, where two curves using refined (a) and waste (b) oil, respectively, are displayed. This results in the conversion abruptly increasing from ~65–99% by using refined oil and by increasing the catalyst amount from 0.5 to 1.0–1.5 g, confirming data discussed in Figure 9. A similar trend was observed with waste oil with an increasing amount of catalyst, with the highest conversion (equal to 94%) achieved in the presence of 1.5 g of catalyst, according to Figure 8. The nonlinearity observed between the biodiesel conversion and catalyst loading was attributed to the heterogeneous nature of the reaction. At a low amount of catalyst, there are not enough active sites for the transesterification reaction [37].

On the other hand, the transesterification reaction performed in the heterogeneous phase needs a long induction time in order to achieve the requested interaction between the reactants and the surface of the catalyst. In this sense, when the plateau is reached, diffusional phenomena are mostly controlling the reaction. Moreover, it cannot be excluded that the catalyst's structure modification occurring during the transesterification reaction affects the conversion behavior [38].

2.3.2. Effect of Catalyst (GRS) Calcination Temperature on the Biodiesel Production

Figure 10 displays the conversion (%) of the refined oil versus the calcination temperature of the natural shell used as the catalyst, at the fixed experimental conditions described previously (5 wt% of catalyst, methanol/oil ratio of 15:1, reaction temperature at the methanol boiling point and 3 h of reaction).
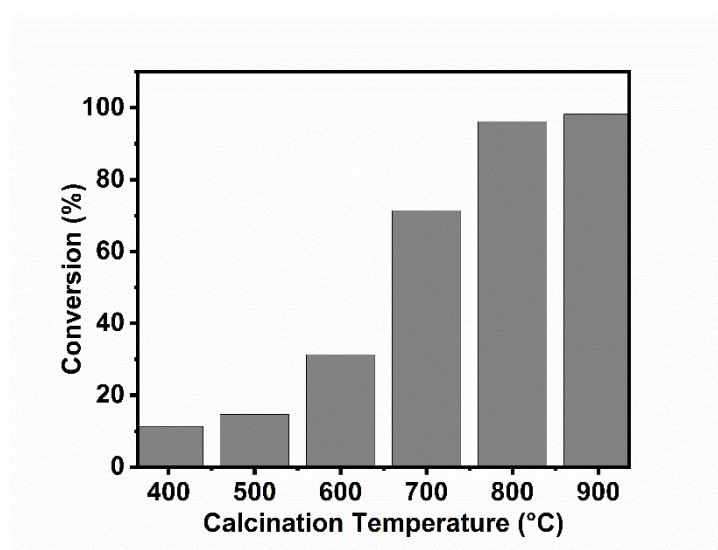

Figure 10. Effect of the catalyst (parent shell) calcination temperature on the biodiesel production using refined oil.

As shown in Figure 10, the conversion slightly increases by increasing the calcination temperature from 400 to 600 °C, then rises quite rapidly by calcining the natural shell in the range of 600–700 °C, and the maximum conversion is reached at 800–900 °C when CaO is formed.

The structural modifications of the GRS as a function of the calcination temperature (see Supplementary Materials, Figure S1) account for the observed behavior.

2.3.3. Catalyst Stability and Recycle

Stability in catalytic conversion and recycling are very important parameters of a heterogeneous catalyst for a wide application [20]. Thus, to test the stability of the catalyst and its use for practical applications, the transesterification reaction was carried out by using waste oil, 5 wt% of the catalyst in the same conditions as previously reported. At the end of each test, the catalyst was filtered, washed with methanol, dried and reintroduced into the reactor. Fresh amounts of oil and methanol were added and allowed to react for a further 3 h at a temperature of 65 °C. This procedure was repeated five times. The results are displayed in Figure 11. In the first catalytic test, 94% of conversion was achieved (according to previously results, as shown in Figure 8, and confirming the reproducibility of experiments); then, the conversion slightly decreased, test by test, up to 87% during the fifth cycle. After that, the recovered catalyst was treated with methanol in an ultrasounds bath for 20 min at the end of each washing step, the powder was filtered and another portion of fresh methanol was added, and the procedure was repeated five times. The XRD characterization (data not shown) of the material washed this way revealed peaks of $Ca(OH)_2$, $CaCO_3$ and CaO; therefore, before a further catalytic test

(sixth cycle), calcination at 900 °C was performed. The biodiesel yield registered in the sixth cycle was as high as 93.6%, quite close to the performance of the freshly used catalyst.
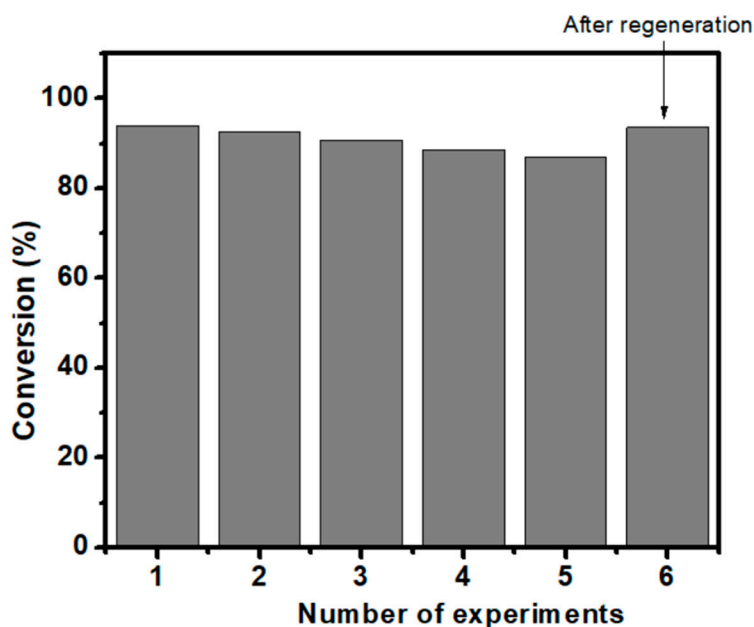

Figure 11. Catalyst reusability tests by using waste oil, 5 wt% of catalyst, at 65 °C and a reaction time of 3 h.

Based on the results reported so far, it can be concluded that the observed deactivation (upon five cycles) was related to the surface modification and blockage of the active sites due to the adsorption of either the reagent (triglyceride molecules), reaction intermediates (diglycerides and monoglycerides) or reaction products. Indeed, according to the literature [24], CaO forms calcium methoxide after reaction with methanol; then, the methoxide reacts with the carbonyl of the triglyceride, forming unstable tetrahedral intermediates that rearrange into the final products, which are three fatty acid esters and a glycerol molecule. Therefore, it is likely that simple washing with methanol is not able to remove the chemisorbed intermediates and reactions products from the catalyst surface, while treatment with bath ultrasounds and further calcination at 900 °C is able to regenerate the pristine active CaO.

For a scale-up of the biodiesel production, one ton of biodiesel forms 50 kg of solid waste catalyst constituted by $Ca(OH)_2$, $CaCO_3$ and CaO. Such solid waste, if not reused as catalyst, is easily recyclable as a construction material.

2.4. Characterization of Synthesized Biodiesel

Table 2 compares the properties of biodiesel produced from used and refined oils with European standards. Apart from the slightly lower yield, all the other parameters are as good as those of biodiesel from refined oil, compliant with European standards [7]. In addition, it should be noted that the currently recognized biodiesel standards have been established for existing diesel engines.

Thus, we cannot exclude that future engines' improvement could allow the use of waste oils for biodiesel production [39].

The biodiesel batches produced by using GRS-derived catalyst were characterized by different techniques. The ^{1}H NMR spectra (Figure 12) show that the proton of the CH-O group of the glycerol appearing usually at 5.3 ppm disappears at the end of the reaction, as well as the fact that no signals at 4.0–4.5 ppm assigned to the protons attached to the triacylglycerols [7] were detected. The strong singlet above 3.66 ppm indicates the formation of the methoxy group of methyl ester ($-CO_2CH_3$). The ^{1}H NMR spectra of the biodiesel samples taken from the waste frying oil do not show any noticeable differences with respect to those from the refined cooking oil. The ester signals resulting from the

OCH$_2$ and OCH groups of triglycerides disappeared, and the signal resulting from the OCH$_3$ ester group of biodiesel appeared at 3.67 ppm, as shown in Figure 12. The assignments of signals in the chemical shift regions of 0.8–3 ppm correspond to those observed in the spectra of the oil samples (see Figure 6).

Table 2. Physico-chemical properties of biodiesel samples obtained from the refined and waste cooking oils.

| Batches' Characteristics		Refined Oil Biodiesel	Waste Oil Biodiesel	European Standards
Maximum biodiesel yield	wt.%	96.5	93.5	-
Ester content	wt.%	97	94.3	≥96.5
Viscosity (40 °C)	mm^2/s	3.5	4.4	3.5–5.5
Density (15 °C)	g/cm^3	0.881	0.908	0.88–0.9
Acid Value	mg KOH/g oil	0.27	0.44	0.5 max
Water content	ppm	348	456	500 max
Sulphur Ash content	mg/Kg	5.6	7.8	10 max
Flash point	°C	130.3	139	120 min
Cetane number		49.5	52.2	51 min
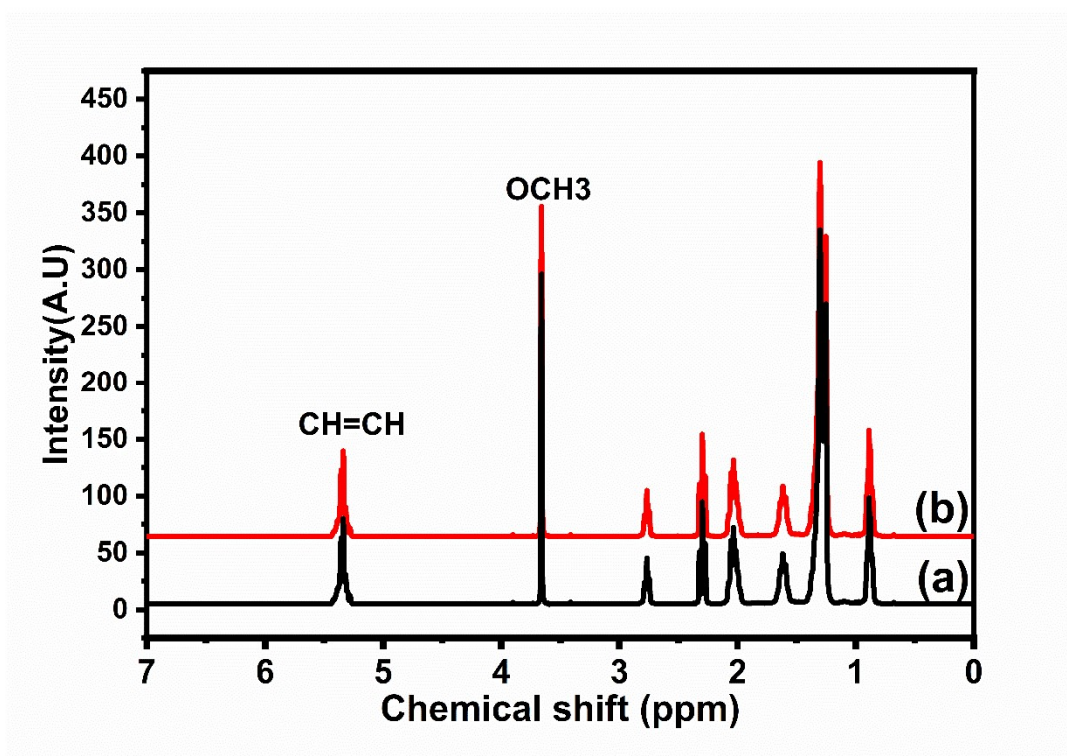
Figure 12. ^{1}H-NMR spectrum of biodiesel obtained with (**a**) refined cooking oil and (**b**) waste cooking oil.

The NMR results were confirmed by FT-IR spectroscopy analysis of biodiesel samples (Figure 13). It is important to note the presence of the band at 1436 cm^{-1}. This band can be selected for biodiesel quantification because it is characteristic of methyl esters (OCH$_3$) [40]. The FT-IR analysis confirmed the high quality of the obtained biodiesel samples independently of the nature of the used feedstock.
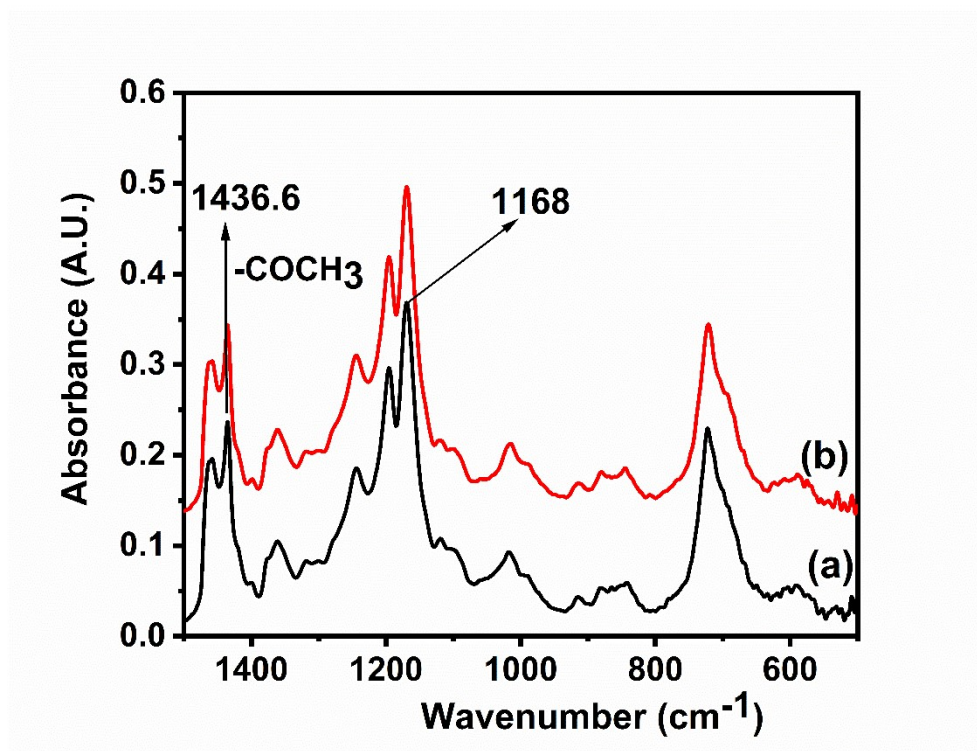
Figure 13. FT-IR spectra of biodiesel obtained with (**a**) refined cooking oil and (**b**) waste cooking oil.

Based on such results, it is plausible that an industrial application of waste earth or marine shells, constituted by calcium and hydrated lime [20,24], could be applied for the large scale synthesis of biodiesel.

3. Material and Methods

3.1. Chemicals and Reagents

Solen marginatus (Grooved Razor Shell) is a bivalve mollusk of the Solenidae family. The animal lives along the shoreline buried in the sand and meets in the low-lying areas and the sublittoral zone. The species occurs from the south of the North Sea to the Mediterranean Sea and the Atlantic coast of North Africa. The shell is thin, fragile and elongated. The dorsal and ventral edges are straights and parallels. The anterior end of the shell truncates obliquely, with a distinct groove on the back and belly near the edge, up to 120 mm long. It feeds by filtration of water retaining food particles, especially plankton.

The other reagents, methanol, ethanol, ethyl ether and KOH, are of analytical grade (Sigma-Aldrich, Darmstadt, Germany) and were used as received.

3.2. Catalyst Preparation

The catalyst was prepared using calcium carbonate in the form of aragonite nanopowder obtained from grooved Razor Shell (GRS), following the method used by Mahmood et al. [21]. The GRS was washed repeatedly with boiling distilled water and dried at 120 °C in an oven. Then, they were crushed into small particles (75 μm). The obtained powder was mechanically stirred with the 50 mL and 0.5 mL of surfactant BS-12 at 1000 rpm at room temperature for 90 min. The resultant slurry was then filtered and dried at 80 °C overnight and then stored in a vacuum desiccator for further use. The catalyst was prepared by calcination of the as-received GRS at temperatures ranging from 100–900 °C.

3.3. Characterization Techniques

X-Ray Diffraction (XRD) patterns were registered by using a powder diffractometer (Shimadzu-6100, Tokyo, Japan) equipped with a variable temperature unit (model HA-1001). In order to investigate the structural modification occurring in the temperature-programmed oxidation mode, the sample material was put in an alumina holder and exposed to CuKα (Kα = 1.54184 Å) radiation (40 kV $\times$ 30 mA) in a continuous temperature step scan operation mode, from 30–900 °C, at a heating rate of 10 °C min^{-1} under air flow (60 mL min^{-1}). Prior to the XRD runs, each sample was kept under isothermal conditions at the selected temperature for 30 min. The samples were analyzed over the angular range of 20–70° 2θ at a scanning speed of 0.02° s^{-1}.

Infrared spectral data were collected by using a VERTEX 70 (Bruker, Milan, Italy) spectrometer equipped with an ATR MIRACLE DIAMANT apparatus (Perkin-Elmer, Milan, Italy). The device has a spectral range of 4000–500 cm^{-1}. The spectra were collected by co-adding 16 scans at a resolution of 4 cm^{-1}.

Simultaneous thermogravimetric/differential thermal analyses (TG/DTA) were carried out on a Labsys TM Evo (1F) Setaram apparatus, by heating from room temperature up to 900 °C with an increasing rate equal to 10 °C·min^{-1}, under air flow (60 mL min^{-1}).

The morphology of the catalyst was investigated by scanning electron microscopy, with a Jeol JSM-7000F FE-SEM, (Jeol, Osaka, Japan). The samples were deposited on carbon grids for analysis.

The physico-chemical and fuel properties, i.e., viscosity, density and acid value of the vegetable oils and produced biodiesel, were determined by the conventional methods (American Society for Testing and Materials (ASTM) methods) and compared with the European standards of biodiesel [41]. The fatty acid concentrations in the raw material and the prepared biodiesel purity were determined to measure their corresponding methyl esters content by a Peri Chrom 2000 gas chromatograph (GC) equipped with a flame ionization detector (FID) and a capillary column DB-WAX (30 m $\times$ 0.32 mm, 0.23-μm film thickness). The detailed method was described previously [7,42].

The oils and transesterification products were also analyzed by NMR, FT-IR and TG/DTA techniques.

The ^{1}H-NMR spectra were recorded at 25 °C with a pulse duration of 30°, a recycle delay of 1.0 s and eight scans by using a BRUKER AVANCE 300 MHz spectrometer (Bruker, Milan, Italy). Deuterated chloroform (CDCl$_3$) was used as a solvent. The ^{13}C NMR (75 MHz) spectra were obtained with a pulse duration of 30°, a recycle delay of 1.89 s and 160 scans. NMR spectroscopy was also used to monitor the transesterification reaction. The conversion is illustrated by the equation given below:

$$C = 100 \times \frac{2A_{Me}}{3A_{CH2}} \tag{1}$$

where:

C = percentage conversion of triglycerides to corresponding methyl esters.
A_{Me} = integration value of the methoxy protons of the methyl esters (3.66 ppm).
A_{CH2} = integration value of α-methylene protons (2.26 ppm).

3.4. Biodiesel Synthesis

The biodiesel laboratory-scale synthesis was performed according to a conventional procedure previously described [7,42]. The refined or waste oil, 100 g, was added under stirring to a mixture of catalyst and methanol at 65 °C, placed in a 250-mL round-bottom glass flask. The use of a reflux condenser prevented methanol evaporation. The resulting mixture was left to react at the temperature of boiling methanol for 3 h. After that, the catalyst was removed by centrifugation, and glycerol was separated from biodiesel after storing the resulting liquid for 8 h in a separating funnel. The unreacted alcohol and water, present in the mixture, were removed under vacuum distillation using a BÜCHI Rotavapor R-114 equipped with BÜCHI Water-bath B-48 (BÜCHI Labortechnik AG, Flawil,

Switzerland). The final product, constituted by methyl esters, was dried at 80 °C and stored before analysis. In order to investigate the catalyst's reusability, catalytic cycles were carried out by using refined oil, 5 wt% of the catalyst, a 65 °C temperature and a reaction time of 3 h. Five consecutive cycles were performed by recovering the catalyst at the end of each test, filtering-washing with methanol, drying and reusing it for a new test. After the fifth cycle, the recovered catalyst was treated with methanol in an ultrasounds bath for 20 min; at the end of each washing step, the catalyst was filtered, a new portion of fresh methanol was added, and the procedure was repeated five times. The catalyst that was regenerated this way was calcined at 900 °C (heating ramp 10 °C min^{-1}) for 1 h and used in a sixth cycle.

4. Conclusions

From the present investigation, the following conclusions can be drawn:

- The optimal conditions for biodiesel production from waste cooking oil collected from Moroccan university restaurants and from refined oil were determined. The raw material that was used was characterized by good properties that were very close to the refined oil used for comparison.
- Calcium oxide obtained by calcination of waste GRS at 900 °C is a good performing catalyst for biodiesel production by the transesterification of waste oil.
- The biodiesel yield reached 94 wt% at a methanol/waste oil ratio of 15:1 and with 5 wt% of catalyst, without any additional cost due to water purification that is necessary when working in homogenous conditions.
- The ^{1}H-NMR, FTIR and gas chromatography analyses of the final product confirmed that: (i) the reaction was complete, and that (ii) the biodiesel samples did not contain any trace of glycerol and (iii) met the required international standards.
- The catalyst, in the form of CaO, was reused for up to five cycles, with a slight decrease in the biodiesel yield from 94–87%. After that, the catalyst was regenerated by washing with methanol in an ultrasounds bath and further calcination at 900 °C for 1 h, recovering an activity very close to that of the fresh catalyst.
- The obtained results can be considered as proof that marine and earth shells can be used as a source of catalysts for biodiesel production.

Author Contributions: This study was conducted through contributions of all authors. A.B.; E.M.L. and M.E.M. equally contributed to the paper, performing experiments and characterizations and writing some parts of the paper. F.O. and A.A. prepared the catalysts. M.K. designed the nature of catalysts and planned the study. L.F.L. contributed to funding the research and completed the writing of the manuscript in its final form. All authors have read and agreed to the published version of the manuscript.

Conflicts of Interest: The authors declare no conflict of interest.

References

1. Van Aalst, M.K. The impacts of climate change on the risk of natural disasters. *Disasters* **2006**, *30*, 5–18. [CrossRef]
2. Hendry, A.P.; Gotanda, K.M.; Svensson, E.I. Human influences on evolution, and the ecological and societal consequences. *Philos. Trans. R. Soc. B Boil. Sci.* **2017**, *372*, 20160028. [CrossRef]
3. Ahuja, D.; Tatsutani, M. Sustainable energy for developing countries. *SAPI EN S. Surv. Perspect. Integr. Environ. Soc.* **2009**, *2*, 1–16.

4. Burke, M.J.; Stephens, J. Political power and renewable energy futures: A critical review. *Energy Res. Soc. Sci.* **2018**, *35*, 78–93. [CrossRef]

5. Hassan, M.; Kalam, M. An Overview of Biofuel as a Renewable Energy Source: Development and Challenges. *Procedia Eng.* **2013**, *56*, 39–53. [CrossRef]

6. Shrirame, H.Y.; Panwar, N.L.; Bamniya, B.R. Bio Diesel from Castor Oil—A Green Energy Option. *Low Carbon Econ.* **2011**, 2, 1–6. [CrossRef]

7. Ouanji, F.; Nachid, M.; Kacimi, M.; Liotta, L.F.; Puleo, F.; Ziyad, M. Small scale biodiesel synthesis from waste frying oil and crude methanol in Morocco. *Chin. J. Chem. Eng.* **2016**, *24*, 1178–1185. [CrossRef]

8. Moreira, K.S.; Júnior, L.S.M.; Monteiro, R.R.C.; De Oliveira, A.L.B.; Valle, C.P.D.; Freire, T.M.; Fechine, P.B.A.; De Souza, M.C.M.; Fernandez-Lorente, G.; Guisan, J.M.; et al. Optimization of the Production of Enzymatic Biodiesel from Residual Babassu Oil (Orbignya sp.) via RSM. *Catalysts* **2020**, *10*, 414. [CrossRef]

9. Hazmi, B.; Rashid, U.; Taufiq-Yap, Y.H.; Ibrahim, M.L.; Nehdi, I. Supermagnetic Nano-Bifunctional Catalyst from Rice Husk: Synthesis, Characterization and Application for Conversion of Used Cooking Oil to Biodiesel. *Catalysts* **2020**, *10*, 225. [CrossRef]

10. Bautista, F.; Aguado-Deblas, L.; Bautista, F.M.; Luna, D.; Luna, C.; Calero, J.; Posadillo, A.; Romero, A.A. Biodiesel at the Crossroads: A Critical Review. *Catalysts* **2019**, *9*, 1033. [CrossRef]

11. Knothe, G.; Steidley, K.R. Kinematic viscosity of biodiesel fuel components and related compounds. Influence of compound structure and comparison to petrodiesel fuel components. *Fuel* **2005**, *84*, 1059–1065. [CrossRef]

12. Conceição, M.M.; Candeia, R.A.; Dantas, H.J.; Soledade, L.; Fernandes, V.J.; Souza, A.G. Rheological Behavior of Castor Oil Biodiesel. *Energy Fuels* **2005**, *19*, 2185–2188. [CrossRef]

13. Jabbari, H. Production of methyl ester biofuel from sunflower oil via transesterification reaction. *Asian J. Nanosci. Mater.* **2018**, *1*, 52–55.

14. Narasimharao, K.; Lee, A.; Wilson, K. Catalysts in production of biodiesel: A review. *J. Biobased Mater. Bioenergy* **2007**, *1*, 19–30.

15. Serio, M.D.; Cozzolino, M.; Giordano, M.; Tesser, R.; Patrono, P.; Santacesaria, E. From Homogeneous to Heterogeneous Catalysts in Biodiesel Production. *Ind. Eng. Chem. Res.* **2007**, *46*, 6379–6384. [CrossRef]

16. Saifuddin, N.; Samiuddin, A.; Kumaran, P. A Review on Processing Technology for Biodiesel Production. *Trends Appl. Sci. Res.* **2015**, *10*, 1–37. [CrossRef]

17. Dall'Oglio, E.L.; Sousa, P.T.D., Jr.; Oliveira, P.T.D.J.; De Vasconcelos, L.G.; Parizotto, C.A.; Kuhnen, C.A. Use of heterogeneous catalysts in methylic biodiesel production induced by microwave irradiation. *Química Nova* **2014**, *37*, 411–417. [CrossRef]

18. Sahu, G.; Gupta, N.K.; Kotha, A.; Saha, S.; Datta, S.; Chavan, P.; Kumari, N.; Dutta, P. A Review on Biodiesel Production through Heterogeneous Catalysis Route. *ChemBioEng Rev.* **2018**, *5*, 231–252. [CrossRef]

19. Sanz-Pérez, E.; Murdock, C.R.; Didas, S.A.; Jones, C.W. Direct Capture of CO2 from Ambient Air. *Chem. Rev.* **2016**, *116*, 11840–11876. [CrossRef]

20. Laskar, I.B.; Rajkumari, K.; Gupta, R.; Chatterjee, S.; Paul, B.; Rokhum, L. Waste snail shell derived heterogeneous catalyst for biodiesel production by the transesterification of soybean oil. *RSC Adv.* **2018**, *8*, 20131–20142. [CrossRef]

21. Mahmood, S.; Bin Abu Bakar, Z.; Razak, I.S.A.; Yusof, L.M.; Jaji, A.Z.; Tijani, I.; Hammadi, N.I. Preparation and characterization of cockle shell aragonite nanocomposite porous 3D scaffolds for bone repair. *Biochem. Biophys. Rep.* **2017**, *10*, 237–251. [CrossRef] [PubMed]

22. Hoque, M.E.; Shehryar, M.; Islam, K.N. Processing and Characterization of Cockle Shell Calcium Carbonate (CaCO3) Bioceramic for Potential Application in Bone Tissue Engineering. *J. Mater. Sci. Eng.* **2013**, *2*, 132. [CrossRef]

23. Khachani, M.; Hamidi, A.E.; Halim, M.; Arsalane, S. Non-isothermal kinetic and thermodynamic studies of the dehydroxylation process of synthetic calcium hydroxide Ca (OH)$_2$. *J. Mater. Environ. Sci.* **2014**, *5*, 615–624.

24. Niju, S.; Begum, K.M.M.S.; Anantharaman, N. Enhancement of biodiesel synthesis over highly active CaO derived from natural white bivalve clam shell. *Arab. J. Chem.* **2016**, *9*, 633–639. [CrossRef]

25. Siriprom, W.; Kaewkhao, J.; Phachana, K.; Limsuwan, P. Crystal Structure and Morphology Dependence of the Phase of Mollusc Shell: A Case Study of XRD, SEM and ESR. *J. Phys. Conf. Ser.* **2011**, *266*, 012124. [CrossRef]

26. Ghafar, S.L.M.A.; Hussein, M.Z.; Rukayadi, Y.; Zakaria, Z.A.B. Surface-functionalized cockle shell–based calcium carbonate aragonite polymorph as a drug nanocarrier. *Nanotechnol. Sci. Appl.* **2017**, *10*, 79–94. [CrossRef]

27. Pelmenschikov, A.G.; van Wolput, J.H.M.C.; Jhchent, P.J.; van Santed, R.A. (A,B,C) Triplet of Infrared OH Bands of Zeolitic H-Complexes. *J. Phys. Chem.* **1995**, *99*, 3612–3617. [CrossRef]

28. Jurac, Z.; Zlatar, V. Optimization of raw material mixtures in the production of biodiesel from vegetable and used frying oils regarding quality requirements in terms of cold flow properties. *Fuel Process. Technol.* **2013**, *106*, 108–113. [CrossRef]

29. Cukalovic, A.; Monbaliu, J.-C.M.; Eeckhout, Y.; Echim, C.; Verhé, R.; Heynderickx, G.; Stevens, C.V. Development, optimization and scale-up of biodiesel production from crude palm oil and effective use in developing countries. *Biomass Bioenergy* **2013**, *56*, 62–69. [CrossRef]

30. Knothe, G.; Kenar, J. Determination of the fatty acid profile by1H-NMR spectroscopy. *Eur. J. Lipid Sci. Technol.* **2004**, *106*, 88–96. [CrossRef]

31. Conceição, M.M.; Candeia, R.A.; Silva, F.C.; Bezerra, A.F.; Fernandes, V.J., Jr.; Souza, A.G. Thermoanalytical characterization of castor oil biodiesel. *Renew.Sustain. Energy Rev.* **2007**, *11*, 964–975.

32. Boey, P.-L.; Maniam, G.P.; Hamid, S.A. Performance of calcium oxide as a heterogeneous catalyst in biodiesel production: A review. *Chem. Eng. J.* **2011**, *168*, 15–22. [CrossRef]

33. Boey, P.-L.; Maniam, G.P.; Hamid, S.A.; Ali, D.M.H. Utilization of waste cockle shell (Anadara granosa) in biodiesel production from palm olein: Optimization using response surface methodology. *Fuel* **2011**, *90*, 2353–2358. [CrossRef]

34. Qasim, D.; Abdul-Aziz, Y.I.; Alismaeel, Z.T. Biodiesel from fresh and waste sunflower oil using calcium oxide catalyst synthesized from local limestone. *Res. J. Chem. Environ.* **2019**, *23*, 111–119.

35. Schuchardt, U.; Sercheli, R.; Vargas, R.M. Transesterification of vegetable oils: A review. *J. Braz. Chem. Soc.* **1998**, *9*, 199–210. [CrossRef]

36. Savaliya, M.L.; Dhorajiya, B.D.; Dholakiya, B.Z. Current Trends in Separation and Purification of Fatty Acid Methyl Ester. *Sep. Purif. Rev.* **2014**, *44*, 28–40. [CrossRef]

37. Al-Muhtaseb, A.; Jamil, F.; Al-Haj, L.; Myint, M.T.Z.; Mahmoud, E.; Ahmad, M.N.; Hasan, A.O.; Rafiq, S. Biodiesel production over a catalyst prepared from biomass-derived waste date pits. *Biotechnol. Rep.* **2018**, *20*, e00284. [CrossRef]

38. Sanchez-Cantu, M.; Perez-Diaz, L.M.; Rosas, I.P.; Cadena-Torres, E.; Juárez-Amador, L.; Rubio, E.; Rodríguez-Acosta, M.; Valente, J.S. Hydrated lime as an effective heterogeneous catalyst for the transesterification of castor oil and methanol. *Fuel* **2013**, *110*, 54–62. [CrossRef]

39. Niculescu, R.; Clenci, A.; Iorga-Siman, V. Review on the Use of Diesel–Biodiesel–Alcohol Blends in Compression Ignition Engines. *Energies* **2019**, *12*, 1194. [CrossRef]

40. O'Donnell, S.; Demshemino, I.; Yahaya, M.; Nwandike, I.; Okoro, L. A review on the spectroscopic analyses of biodiesel. *Eur. Int. J. Sci. Technol.* **2013**, *2*, 137–146.

41. Tariq, M.; Shahzadi, S.; Ahmad, F.; Ahmad, M.; Zafar, M.; Khalid, N.; Khan, M.A. Identification, FT-IR, NMR (1H and 13C) and GC/MS studies of fatty acid methyl esters in biodiesel from rocket seed oil. *Fuel Process. Technol.* **2011**, *92*, 336–341. [CrossRef]

42. Kara, K.; Ouanji, F.; El Mahi, M.; Lotfi, E.M.; Kacimi, M.; Mahfoud, Z. Biodiesel synthesis from vegetable oil using eggshell waste as a heterogeneous catalyst. *Biofuels* **2019**, 1–7. [CrossRef]